Discrimination by EIS of Degradation Mechanisms in Lap Joints of Coated Metal Sheet

A. Bautista, J.A. González, E. Otero, M. Morcillo—Centro Nacional de Investigaciones Metalúrgicas, CSIC* and E. Almeida—Instituto Nacional de Engenharia e Tecnologia Industrial (INETI)†

The information derived from impedance diagrams obtained by using electrochemical sensors specifically designed for lap joints testing of coated metallic sheets is analyzed. The electrochemical sensors were made by means of steel or zinc sheets, uncontaminated or contaminated with variable amounts of sodium chloride, and overcoated with organic coatings. Such sensors show the effect of the nature of the metallic substrate, the underfilm saline contamination, and the relative humidity of the environment outside the lap joint.

The results show that the information obtained from electrochemical impedance spectroscopy (EIS) on the behavior within the lap joints can be assessed by the criteria traditionally used for plain painted metal surfaces.

By modeling the data, it is possible to discriminate between effects due to the organic coating and to the corrosion reaction at the metal-coating interface.

INTRODUCTION

Electrochemical impedance spectroscopy (EIS) is the most widely used technique for characterizing protective organic coatings applied to metal surfaces.[1-14] However, the rather variable shape of impedance diagrams and the large number of corrosion factors involved in painted metal/medium systems severely complicates the interpretation of impedance data.

Figure 1 shows a non-exhaustive scheme of the main factors related to the three phases that make up such systems, viz., an aggressive medium, an organic coating, and a metal substrate. One must also consider the exchanges between phases that take place across the two interfaces present in these heterogeneous systems.

The situation is further complicated by the fact that the properties of each phase are not completely independent. Thus, the barrier effect of the coating depends directly on its thickness and on the composition and structure of the constituent polymer, and indirectly on the coating's adhesion to the substrate and osmotic phenomena. The adhesion in turn is a function of the nature and roughness of the metal surface and the type of coating, whereas the effect of osmotic phenomena is dependent on the presence and concentration of ions in the medium and the coating under it.[6]

The electrochemical nature of corrosion calls for a permanent electrolyte or an occasional one such as the atmosphere, which contains condensable components. In the latter case, the presence of lap joints can accelerate the deterioration of the protective system by facilitating condensation and significantly increasing the wetting time inside crevices. The experimental difficulties involved in applying electrochemical techniques to lap joints can be overcome by using suitable electrochemical sensors.[7]

Corrosion at the metal-coating interface involves the prior penetration of water, oxygen, and ions in the bulk medium through coating defects (*Figure* 2a); or by their diffusion or reaction with the coating leading to their incorporation into the coating's structure in non-defective coatings (*Figure* 2b). When the electrolyte reaches the interface, the EIS technique can provide information about its behavior; such information is interpreted in the light of equivalent circuits (EC) that reproduce the potential responses of the system.

Most of the impedance spectra obtained in painted metals can be explained by the EC depicted in *Figure* 3a and its variations.[3-10] In this EC, which reproduces the behavior of defective coatings (*Figure* 2a), R_e denotes the resistance of the electrolyte or corrosive solution, R_{po} the

*Avda. Gregorio del Amo ns 8, 28040-Madrid, Spain. E-mail: abarija@cenim.csic.es.
†Estrada do Paço do Lumiar, 1699-Lisboa Codex, Portugal.

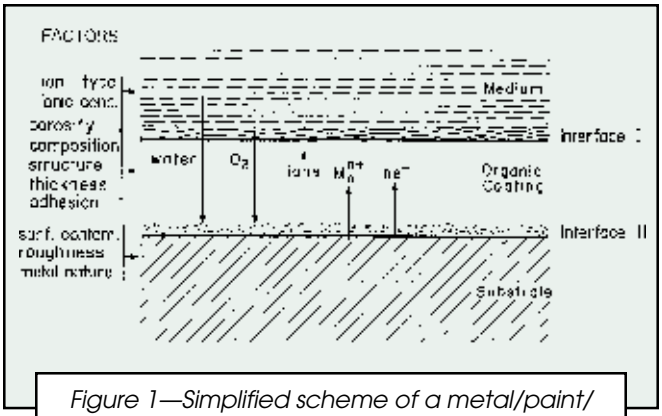

Figure 1—Simplified scheme of a metal/paint/aggressive medium system.

resistance of the pores in the protective organic coating, C_c its capacitance, R_t the charge-transfer resistance of the corrosion process and other reactions potentially occurring at the metal-coating interface, C_{dl} the double-layer capacitance of the interface and W the impedance associated with diffusive mass transfer (the Warburg impedance). In this EC model, the defects and intact areas of the coating are in parallel to each other, and the defective fraction of the coating surface is in series with the corrosion reaction at interface II and with potential diffusive mass transfer phenomena, represented by the Warburg impedance. When R_{po}, which represents the barrier effect of the coating, is very large, the whole current circulates through C_c and the EC of *Figure* 3a simplifies to that of *Figure* 3b. In non-defective coatings, the resistance and capacitor, which represent the coating and interfacial reactions, must be arranged serially (*Figure* 3c) rather than in parallel.

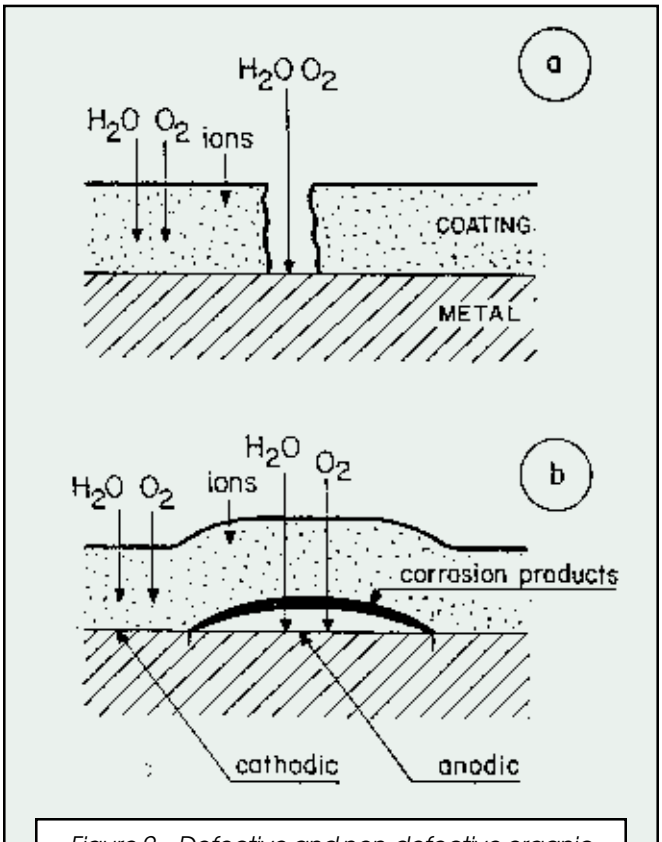

Figure 2—Defective and non-defective organic coatings.

The electrochemical behavior within the typical crevices of lap joints can thus be derived from EIS diagrams, with specially designed electrochemical sensors.[7] Can such information be assessed as per the criteria traditionally used in the characterization of painted metal systems? The principal aim of this work is to provide an answer to this question.

EXPERIMENTAL

We used the sensor types depicted in *Figures* 4 and 5, with free and overlapped surfaces. All measurements were made by using a PAR 273A potentiostat and a Solartron 1251 transfer function analyser.

The sensors corresponding to *Figure* 4 were fabricated with low-carbon and zinc 99.9% purity plates coated with a 10 μm dry film thickness transparent lacquer. The sensor was assembled overlapping two uneven plates of 10×2 cm and 10×5 cm, thus the overlapping area was 10×2 cm^2. In this way, the outer surface of the lap joint enables the cathodic semireaction, as occurs in practice. One plate was used as a working electrode (WE) and the other as both a counterelectrode (CE) and reference electrode (RE) during measurements.

The effect of underfilm contamination in both types of substrate was checked by applying the transparent lacquer over clean surfaces and over surfaces that had previously been contaminated with 50 or 500 mg NaCl/m^2. The sensors of *Figure* 5 were used to analyze galvanized steel plates that were industrially prepainted. The protective system comprised a gray polyester primer on one side and the primer plus a finishing white polyester layer on the other.

Both the primer coating and the total protection coating (primer plus finishing layer) were tested for variable lengths of time up to 30 days; joints were disassembled to make impedance measurements in the occluded zones and reassembled immediately afterwards. Following each measurement, the sensors were immersed in distilled water in order to wet the whole overlapping surface by capillarity; between measurements, the sensors were stored in small chambers at a very high relative humidity.

RESULTS

The impedance spectra obtained for both the industrially prepainted galvanized specimens and the Fe and Zn specimens to which a 10 μm thick film of transparent lacquer was applied conformed to one of the three models depicted in *Figure* 6 depending on the different corrosion factors considered in each case. As can be seen from the curves a in *Figure* 6, when the organic coating acts as a highly efficient barrier against water and oxygen penetration, a capacitive behavior is observed throughout

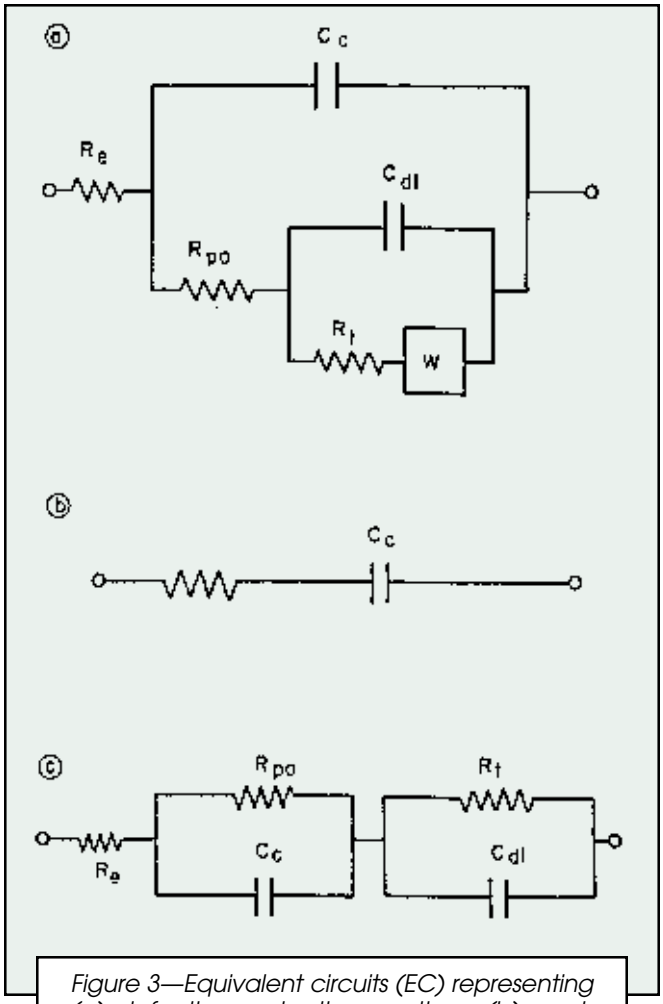

Figure 3—Equivalent circuits (EC) representing (a) defective protective coatings; (b) coatings with a high barrier effect; and (c) non-defective coatings.

the frequency range—at least up to 10^9 Ω cm^2, which is the upper limit for precise measurements with the experimental set-up used. Curves a were obtained for uncontaminated Fe sensors, clamping the two coated plates together only during the impedance measurements (discontinuous lapping, DL in *Figure* 6). As the efficiency of the barrier effect declines, responses consist of a single semicircle in the Nyquist diagram, with impedances in the region of 10^7 Ω cm^2 as shown by the curves b of *Figure* 6, obtained for continuous lapping (CL) of uncontaminated Zn plates. Subsequently, as the protective coating degrades, the diagrams consist of two semicircles with Z values normally below 10^6 Ω cm^2 at low frequencies, as is shown in curves c of *Figure* 6, obtained for continuous lapping of contaminated Zn plates. When the protective system is extensively deteriorated, the impedance spectra occasionally include a third, usually ill-defined semicircle resulting from a high dispersion in the low-frequency data (*Figure* 7).

By contrast, extensively corroded Fe specimens coated with transparent lacquer frequently give rather different impedance diagrams (*Figure* 8).

The effects of each corrosion factor were studied by keeping all other experimental factors constant. By way of example, *Figure* 9a shows temporal changes in R_{po} and R_t, and *Figure* 9b those in C_c, for Zn specimens coated with a 10 µm film of lacquer (over a clean surface or one contaminated with 500 mg/m^2 NaCl). In the absence of underfilm contamination (uncontaminated continuous lapping, CLu), the Nyquist diagram contains a single semicircle that allows R_{po} and C_c—but neither parameter related to the interfacial reaction—to be determined. Contaminated sensors (CLc) give Nyquist diagrams with two semicircles that allow R_t and C_{dl} to be estimated as well. As can be seen, R_{po} varies over much wider ranges than does C_c. The sustained increase in R_{po} over the first 35 days in the test involving continuous lapping of two uncontaminated Zn plates, can be ascribed to gradual drying of the inner overlapped surfaces. The abrupt decrease from the 35th to 36th day was obtained after immersion of the sensor during 15 min in distilled water to restore the initial moistening degree. The results illustrate the effect of underfilm contamination and the moistening degree of the lap joint on the properties of the protective coating and on interfacial processes.

DISCUSSION

The electrochemical parameters that can be estimated from the high-frequency semicircle in a Nyquist dia-

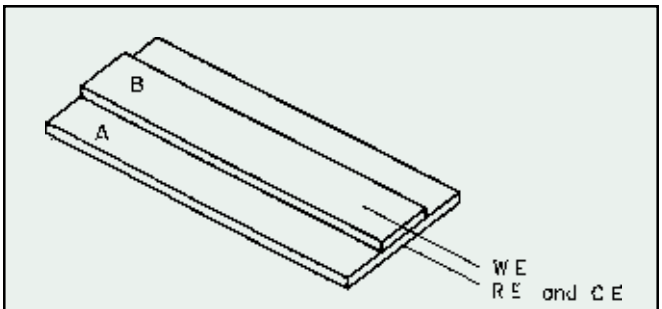

Figure 4—Electrochemical sensor for studying the behavior of lap joints using the dual electrode technique. WE, RE and CE denote working, reference and counter-electrode, respectively.

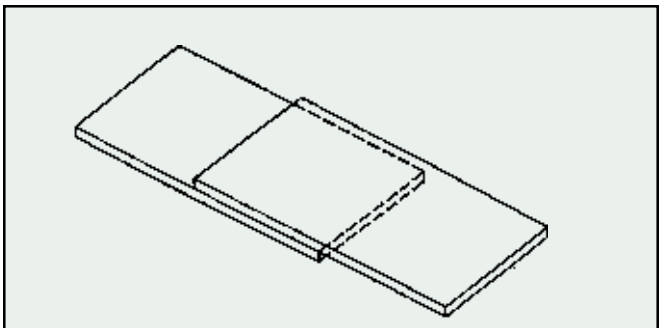

Figure 5—Electrochemical sensor for studying the behavior of lap joints that is disassembled for measurements.

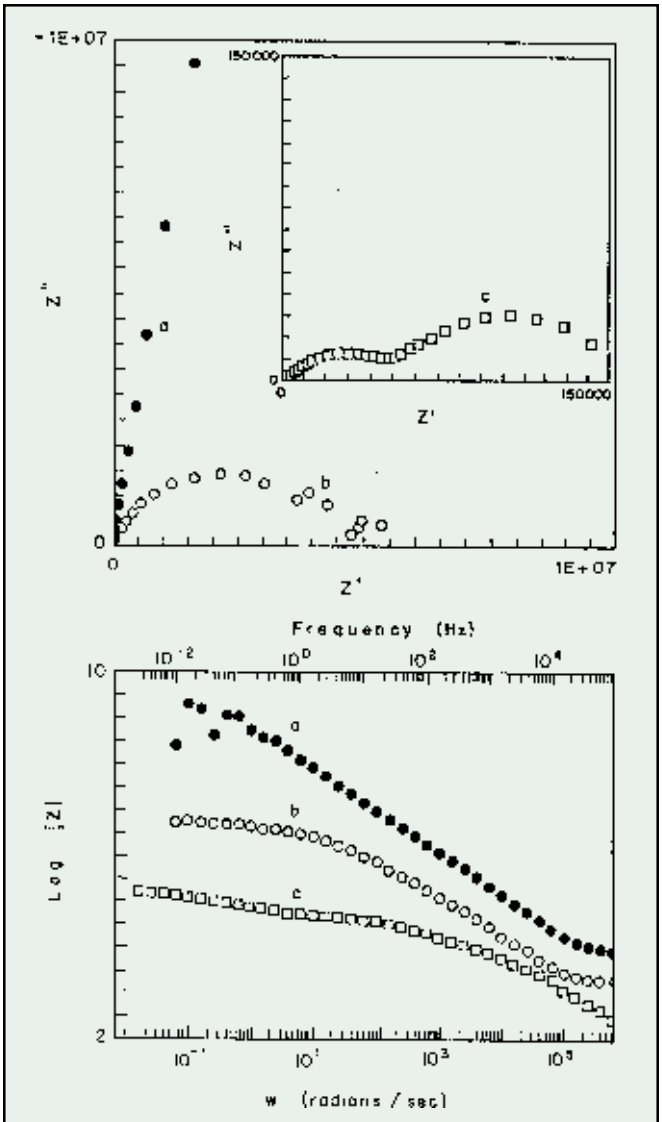

Figure 6—Typical behavior of painted metals as determined by EIS. (a) Perfect barrier effect (●); (b) moderate barrier effect (❍); and (c) weak barrier effect (❑).

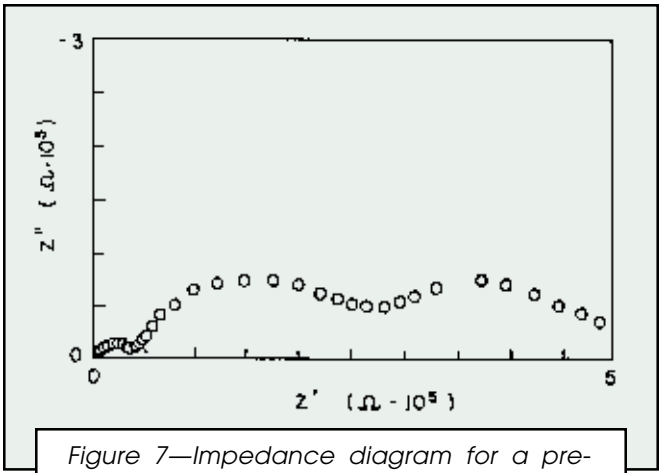

Figure 7—Impedance diagram for a pre-painted galvanized Zn roof that exhibited rusty spots after two years of service life.

gram, R_{po} and C_c, relate to the protective coating system, whereas those derived from the low-frequency semicircle, R_t and C_{dl}, relate to corrosion or other types of interfacial reaction.

The products $R_{po}\bullet C_c$ and $R_t\bullet C_{dl}$, both of which are given in seconds ($V\ cm^2/A \times A\ s/V\ cm^2$), are rough estimates of the time constants T_1 and T_2 associated to both semicircles.

When a single semicircle is obtained, the question arises as to whether the parameters derived from the impedance diagram correspond to the coating or to interfacial corrosion. Under these circumstances, the following considerations may be of assistance:

(1) When the coating is in good condition, R_{po} can be large enough to act as a perfect barrier that will force the current to circulate through C_c during electrochemical measurements. A capacitive behavior is observed as a result with impedances inversely proportional to the frequency up to $10^9\ \Omega$—the upper limit of the equipment used (*Figure* 6, curves a).

(2) As water gradually incorporates into the coating, R_{po} decreases and the situations depicted in curves b and c of *Figure* 6 occur (i.e., one and two semicircles, respectively, in the Nyquist diagram).

(3) With a single semicircle, if its diameter defines a resistance above $10^6\ \Omega\ cm^2$, then it must correspond to R_{po} since R_t is usually smaller—except in passive metals, which require no protective coating.

(4) At $R \ll 10^6\ \Omega\ cm^2$, the barrier effect is very weak and the measured resistance may correspond to a deteriorated coating, a corrosion reaction involving a significant fraction of the substrate surface or a combination of both. Because C_c will be very small (in the nanofarad region or below) and C_{dl} is usually several order of magnitude greater than C_c, in the order of $10^{-5}\ F\ cm^{-2}$,[2] the estimated value of the capacitance frequently dispels the doubt.

(5) The semicircle diameter is dependent on polarization if a charge-transfer phenomenon is involved and

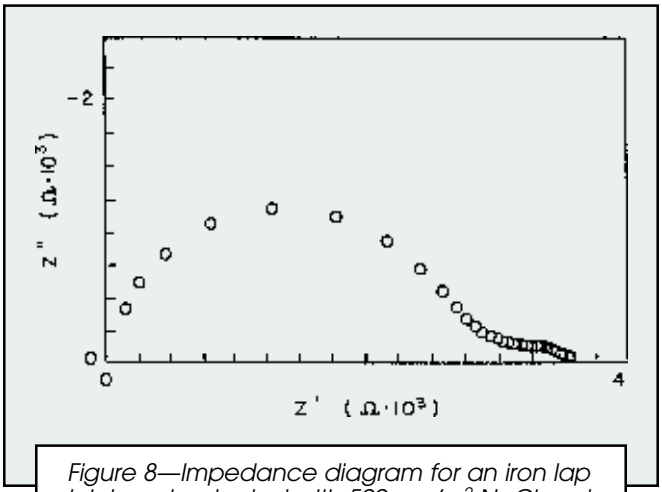

Figure 8—Impedance diagram for an iron lap joint contaminated with 500 mg/m² NaCl and protected by a 10 μm thick film of transparent lacquer, obtained after 100 hr or standing in a wet chamber.

independent of it if it corresponds to the ionic conductivity of the coating[8]—this entails further testing, however.

Before both semicircles become well defined, a transient situation where the two time constants are fairly similar occurs; the result is a single semicircle that encompasses the information on the protective system and on the interfacial reaction; its diameter is the sum of R_{po} and R_t. Let us consider this situation for a defective coating (*Figure* 2a).

Corrosion Under Defective Coatings

Consider a steel specimen bearing a coating with a defective area fraction θ. R_{po} and R_t should theoretically be inversely proportional to θ and related to each other. On the other hand, C_{dl} should increase with increasing θ and C_c should be virtually constant except at high θ values. If one assumes C_c to be approximately 10^{-9} F cm^{-2}, water resistivity (ρ) to be ca. 10^6 Ω cm, R_t for bare steel to be 10^4 Ω cm^2, C_{dl} to be in the order of 10^{-5} F cm^{-2}, and the thickness of the paint coating to be 100 µm, then the foreseeable theoretical situations occurring as a function of the proportion of coating surface defects will be those shown in *Table* 1. While θ is very small (< 0.1%), only a single semicircle of diameter $R_{po} + R_t$ appears and C_{dl} is similar to C_c or even smaller, so the information pertains virtually exclusively to the coating.

At significant θ values (≥ 0.1), the decreased R_{po} value allows the passage of current through it and, hence, through R_t or C_{dl} (*Figure* 3a), so the information obtained pertains also to the interfacial reaction. As can be seen from *Figure* 10, the result of using the EC in *Figure* 3a to simulate some of the systems described in *Table* 1, gives Nyquist diagrams containing a single semicircle at θ values up to 0.1; at θ = 1, however, the diagram already contains two well-defined semicircles and the two time constants are clearly different (T_2/T_1 = 100). The two semicircles are much better resolved at substantial deterioration levels (e.g., θ = 10, where T_2/T_1 = 1000). Some authors claim that, for the two time constants to be visually resolved into two semicircles, one must be at least 20 times greater than the other, and the resistances must be similar to each other—neither should be more than five times higher than the other.[11]

In the Zn specimens subject to underfilm contamination (*Figure* 9a), where the two semicircles in the Nyquist diagram appear after a short initial period, the two time constants differ by several orders of magnitude (*Figure* 11). T_1 usually decreases markedly as the coating deteriorates—in parallel with R_{po}; on the other hand, C_c scarcely changes. This accounts for the markedly decreased value of T_1 in the presence of underfilm contamination, consistent with *Figure* 11.

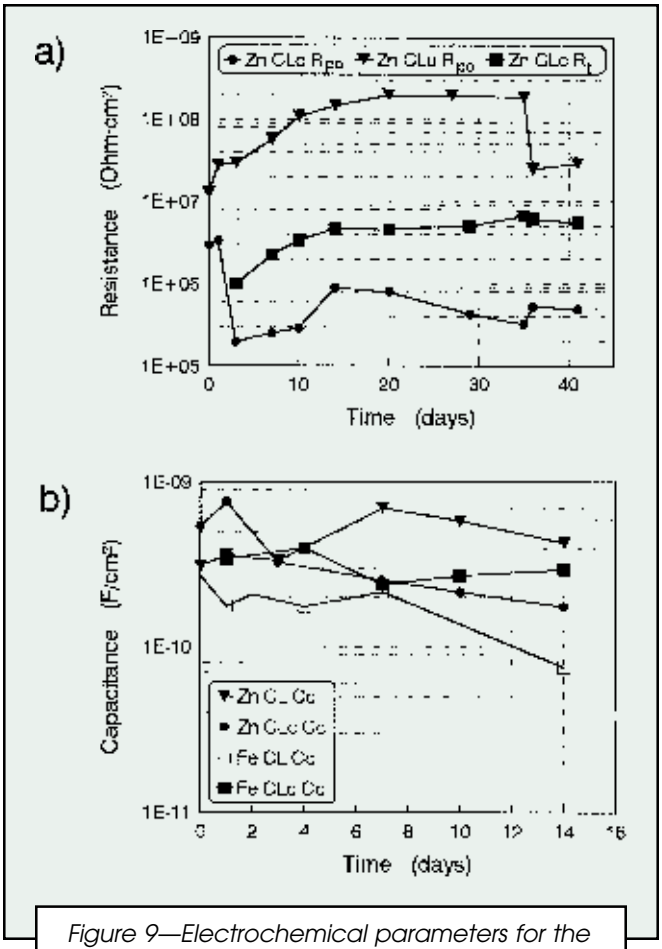

Figure 9—Electrochemical parameters for the coating and the substrate's charge-transfer reaction in contaminated and uncontaminated Zn sensors. (a) Resistances, and (b) coating capacitances.

Information About the Coating's Properties

For practical purposes, in a metal/paint/aggressive medium system, the protective properties of the coating and its durability under the effect of the medium are of greater interest than is substrate corrosion, since the latter entails some previous failure in the coating (viz., a more or less marked loss of its barrier effect).

Table 1—Parameter Values Predicted for the Interfacial Reaction and the Coating as a Function of the Coating's Extent of Deterioration (θ)

θ (%)	R_{po} (Ω)	T_1 (s)	R_t (Ω)	C_{dl} (F/cm^2)	T_2 (s)	T_1/T_2
0.001	10^9	1.0	10^9	10^{-10}	0.1	0.1
0.01	10^8	10^{-1}	10^8	10^{-9}	0.1	1
0.1	10^7	10^{-2}	10^7	10^{-8}	0.1	10
1	10^6	10^{-3}	10^6	10^{-7}	0.1	10^2
10	10^5	10^{-4}	10^5	10^{-6}	0.1	10^3
100	—	—	10^4	10^{-5}	0.1	

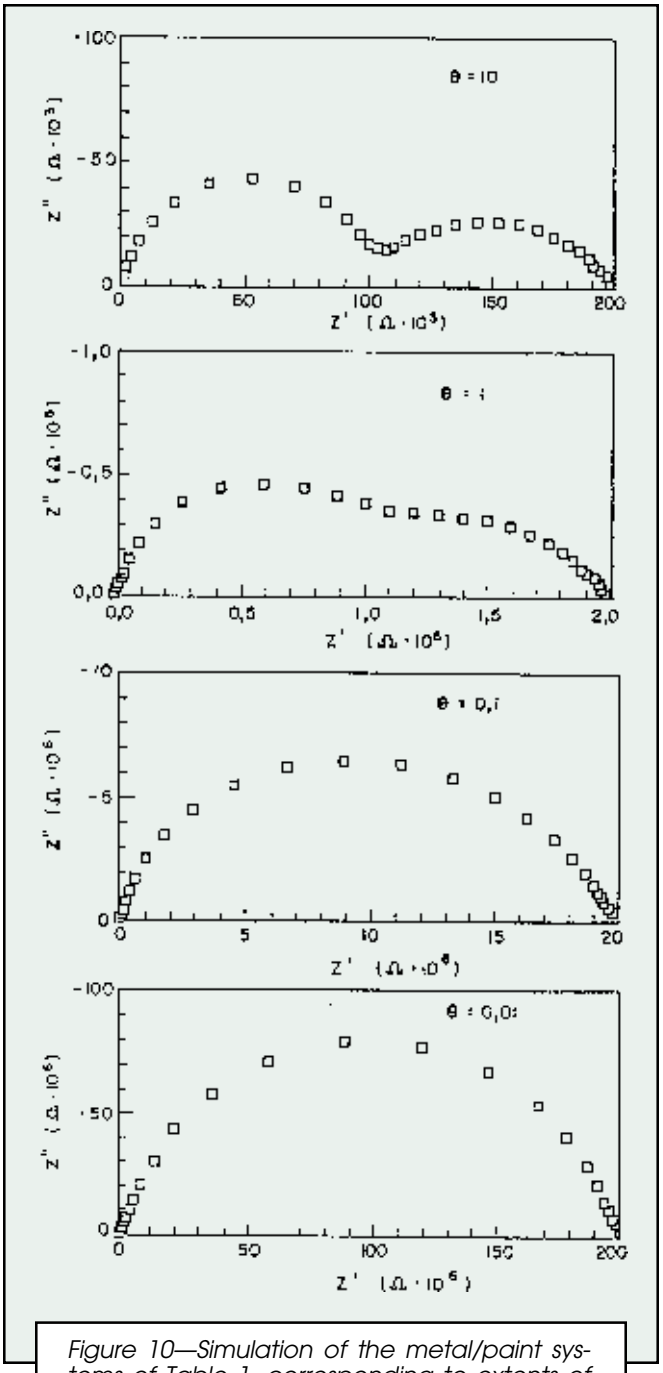

Figure 10—Simulation of the metal/paint systems of Table 1, corresponding to extents of deterioration, θ, of 10, 1, 0.1 and 0.01%, by using the EC of Figure 3a.

Of the two elements in the EC of *Figure* 3a that are related to the coating, R_{po} and C_c, the former varies over a much wider range than the latter. Consequently, R_{po} is a much more sensitive means for assessing the extent of deterioration or how rapidly it develops than is C_c (*Figures* 9a and 9b). C_c depends on the relative dielectric constant of the coating polymer (ε), that of vacuum (ε_0), the coating thickness (d), and the area involved in the measurement (S):

$$C_c = \frac{\varepsilon_0 \varepsilon S}{d} \quad (1)$$

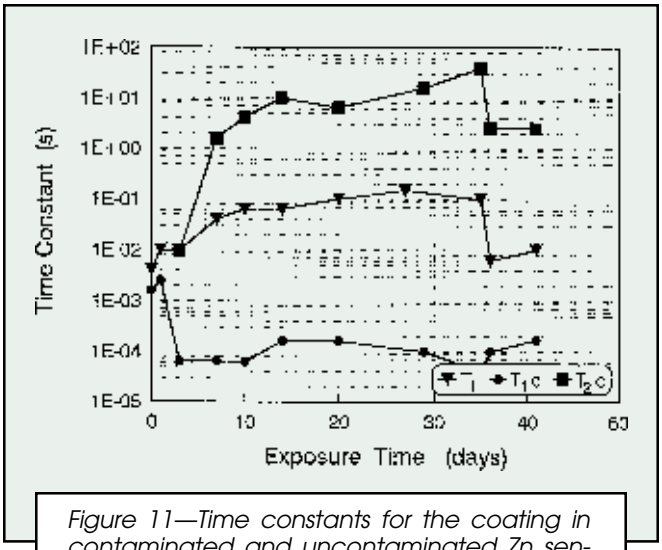

Figure 11—Time constants for the coating in contaminated and uncontaminated Zn sensors (T_1c and T_1, respectively) and for interfacial reaction in presence of underfilm contamination (T_2c) under the conditions of Figure 9a.

Because ε for water (80) is much larger than the typical values for polymers, its temporal variation (derived from C_c as evaluated from the impedance diagrams) can be used to estimate the way water incorporates into the coating.[6] However, the absorption of water by the coating also alters R_{po}—and to a much greater extent than C_c (*Figures* 9a and 9b).

Some authors determine the loss factor (tan δ, where δ is the complement to the dephase angle at a frequency of 1 kHz) after 24 hr of exposure of the coating to the aggressive medium as an expeditious method for assessing the protective power of coatings.[12,13] The loss factor is defined by the ratio between the loss current and the storage current in a dielectric as the protective organic coatings.[12] If tan δ < 0.2 after 24 hr of exposure, then the protective

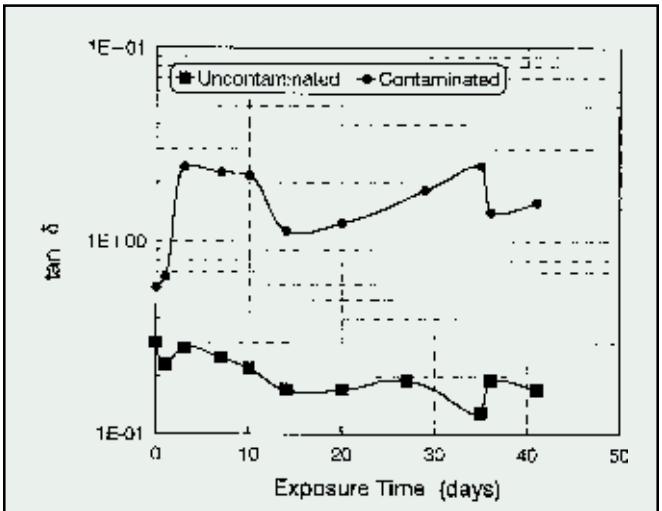

Figure 12—Variation of the loss factor, tan δ, with time under the same conditions as in Figure 9a.

system concerned will be highly resistant to the atmosphere.[13] The loss factor increases as coating durability decreases. As can be seen from *Figure* 12, constructed from the same impedance diagrams as *Figure* 9a, the adverse effect of underfilm contamination can be predicted from the loss factor.

One other qualitative measure similar to the loss factor is the frequency corresponding to a dephase angle of 45°, called the "break point frequency," f_{bp},[2,5] where the real and imaginary components of the impedance become equal. *Figure* 13 shows the temporal variation of this parameter under the same conditions used to determine the loss factor in *Figure* 12. The similarity between the two figures suggests that both procedures are seemingly equivalent.

Both measures, which can be used for the simple, expeditious prediction of the relative behavior of different coatings towards a common medium, or the response of a given coating to different media, rely on the assumption that, the smaller the time constant $T_1 = R_{po} C_c$ (and hence the barrier effect of the coating), the larger will be tan δ or the break point frequency (f_{bp}).

However, provided the high-frequency semicircle in the Nyquist diagram is well-defined, the R_{po} value determined from it provides the same qualitative information as tan δ or f_{bp} and also a quantitative measure of the coating's resistance to deterioration. None of these quantities, however, is a measure of corrosion rate.

Information Provided by Interfacial Reactions

The presence of a second semicircle in the impedance diagrams suggests some prior decline in the barrier effect of the coating; for practical purposes, the relative times required for a given extent of deterioration to be reached under different conditions is more interesting than the absolute values of R_t and C_{dl}. If the response of the bare metal to the same medium is known, R_t and C_{dl} will provide a measure of the corrosion state of the system rather than of its corrosion kinetics. If R_{tu} and C_{dlu} are used to denote the values for the unprotected substrate, then the following relations must hold:

$$\theta = \frac{R_{tu}}{R_t} \qquad (2)$$

$$\theta = \frac{C_{dl}}{C_{dlu}} \qquad (3)$$

For simplicity, the impedance at a low frequency (e.g., 1 mHz) is proposed as a quantitative estimate for the transfer resistance. Several ac monitors based on simplified impedance measurements over different frequency ranges have become available.[14] This simplification is much more suitable for bare metals than for painted metals since the low-frequency impedance coincides roughly with R_{po} while the barrier effect is still strong (with $Z = 1/\omega C$ at extremely high R_{po} values) and approaches R_t when the coating is extensively deteriorated [e.g., under the effect of underfilm contamination (*Figure* 14)]. Complementary measurements of the loss factor, tan δ, may allow one to determine whether Z_{1mHz} is primarily due to the coating's barrier effect or the charge-transfer reaction.

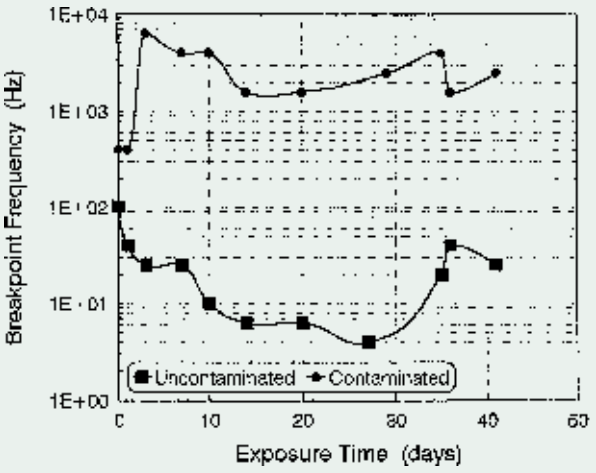

Figure 13—Variation of the break point frequency, f_{bp}, with time under the same conditions as in Figure 9a.

Corrosion Under Non-Defective Coatings

When corrosion occurs under a non-defective coating (by diffusion of the electrolyte through the coating's polymer or incorporation of the electrolyte into the polymer structure), impedance data must be interpreted according to markedly different criteria. In fact, this situation conforms more closely to the EC of *Figure* 3c than to that used so far (*Figure* 3a).

When a single semicircle of diameter $\phi > 10^6\ \Omega cm^2$ appears in the Nyquist diagram, the resistance is highly likely to result from the coating, thus suggesting a strong barrier effect of the protective system. At long exposure

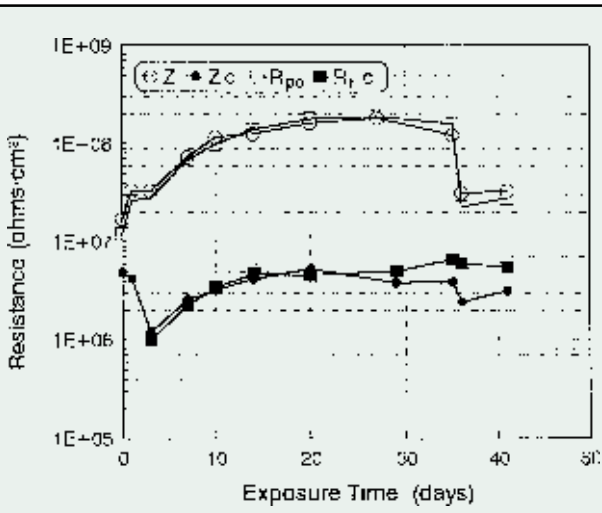

Figure 14—The impedance at 1 mHz provides accurate estimates of the ionic resistance of the coating (R_{po}) in uncontaminated Zn sensors (Z) and of the charge-transfer resistance (R_t) in the presence of underfilm contamination (Z_c).

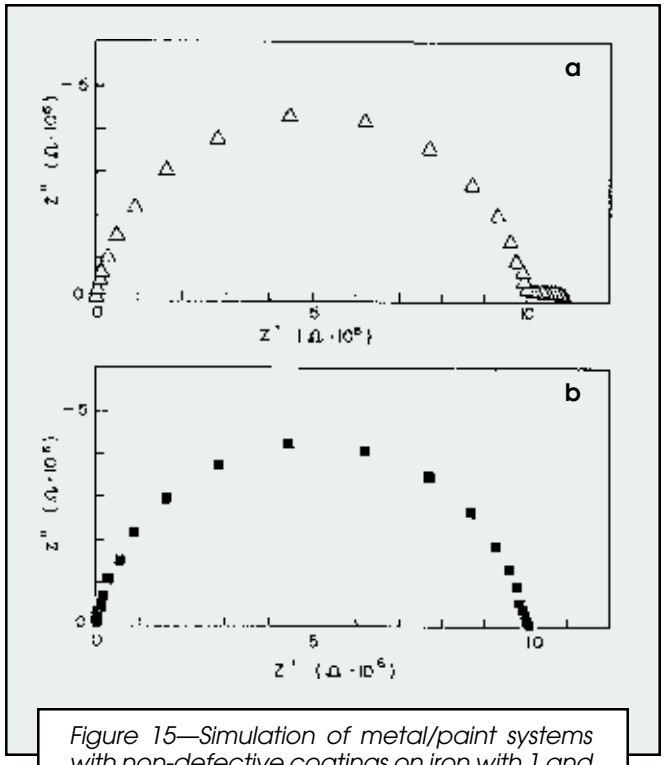

Figure 15—Simulation of metal/paint systems with non-defective coatings on iron with 1 and 10% of the metal area corroded. (a) $C_c = 10^{-10}$ F cm^{-2}, $R_{po} = 10^7$ Ω cm^2, $R_t = 10^6$ Ω cm^2 and $C_{dl} = 10^{-6}$ F cm^{-2}; and (b) $C_c = 10^{-10}$ F cm^{-2}, $R_{po} = 10^7$ Ωcm^2, $R_t = 10^5$ Ω cm^2 and $C_{dl} = 10^{-5}$ F cm^{-2}.

times—and also at short times in the presence of underfilm contamination—R_t may be much less than R_{po}—in fact, the interfacial reaction usually goes unnoticed in impedance diagrams when the risk of substrate corrosion at the interface is maximal. *Figure* 15, constructed by simulation from the EC of *Figure* 3c, shows this type of situation at two different degrees of surface corrosion (1 and 10%, which correspond to R_t values of 10^6 and 10^5 Ω cm^2, respectively) for a coating of $R_{po} = 10^7$ Ω cm^2. The impedance diagrams obtained are similar to those encountered in practice in studying the behavior of steel contaminated with 500 mg/m^2 NaCl and then coated with a 10 µm thick film of transparent lacquer (*Figure* 8). In uncertain situations, the appearance of the samples can be of great assistance in correctly interpreting impedance data; e.g., the specimen of *Figure* 8 exhibited an extensively corroded surface. The presence of blisters or a markedly decreased adherence of the coating can be valuable indicators in this respect.

Rather than the absolute value of R_t or C_{dl}, the time they take to become apparent and their subsequent changes can provide valuable clues, particularly for comparative purposes, when a given corrosion factor is altered on constancy of all other conditions.

CONCLUSIONS

The results obtained in this work allow us to draw the following conclusions:

(1) Specifically designed electrochemical sensors can be used to obtain comprehensive information on the metallic corrosion mechanism and on the protective coating deterioration process within the lap joints

(2) Such information can be assessed by the criteria traditionally used in the characterization of plain painted metal surfaces.

(3) Parameters such as the loss factor, the break point frequency, and the pore resistance of the organic coating, can be used as simple and rapid indicators for predicting the relative behavior of coated metallic sheets in lap joints.

References

(1) Bastidas, J.M., Cabañes, J.M., and Catalá, R., "Effect of Passivation Treatment and Storing on Adhesion and Protective Properties of Lacquered Tinplate Cans," Journal of Coatings Technology, *69*, No. 871, 67 (1997).
(2) Hepburn, B.J., Gowers K.R., and Scantlebury, J.D., "Interpretation of Low Frequency AC Impedance Data for Organic Coatings on Mild Steel," *Br. Corros. J.*, 21, No. 2, 105 (1986).
(3) Amirudin, A. and Thierry, D., "Application of Electrochemical Impedance Spectroscopy to Study Efficiency of Anticorrosive Pigments in Epoxy-Polyamide Resin," *Br. Corros. J.*, 30, No. 2, 128 (1995).
(4) Walter, G.,"A Review of Impedance Plot Methods Used for Corrosion Performance Analysis of Painted Metals," *Corros. Sci.*, 26, No. 9, 681 (1986).
(5) Feliu, S., Galván, J.C., and Morcillo, M., "The Charge Transfer Reaction in Nyquist Diagrams of Painted Steel," *Corros. Sci.*, 30, No. 10, 989 (1990).
(6) Geenen, F., "Characterization of Organic Coatings with Impedance Measurements," Ph. Thesis, Technische Universiteit Delf, Netherland, September 1991.
(7) González, J.A., Bautista, A., Otero, E., Morcillo, M., and Almeida, E., "Use of Electrochemical Impedance Spectroscopy for Studying Corrosion at Overlapped Joints," *Prog. Org. Coat.*, 33, No. 1, 61 (1998).
(8) Bonora, P.L., Deflorian, F., and Fedrizzi, L., "Electrochemical Impedance Spectroscopy as a Tool for Investigating Underpaint Corrosion," *Electrochim. Acta*, 41, Nos 7/8, 1073 (1996).
(9) Mansfeld, F. and Kendig, M.W., "Electrochemical Impedance Spectroscopy of Protective Coating," *Werkst. Korros.*, 36, No. 11, 473 (1985).
(10) Thompson, I. and Campbell, D., "Interpreting Nyquist Responses from Defective Coatings on Steel Substrates," *Corros. Sci.*, 36, No. 1, 187 (1994).
(11) Walter, G.W., "Application of Impedance Measurements to Study Performance of Painted Metals in Aggressive Solutions," *J. Electroanal. Chem.*, 118, 259 (1981).
(12) Sato, Y., "Mechanism and Evaluation of Protective Properties of Paints," *Prog. Org. Coat.*, 9, 85 (1981).
(13) Petrovich, I., Bastidas, J.M., Morcillo, M., and Feliu, S., "Comportamiento de un Recubrimiento de Pintura Sobre Acero Galvanizado. Aplicación de la Técnica de Impedancia," *Rev. Iberoam. Corros. Prot.*, 14, No extra., 219 (1983).
(14) Hladky, K., Callow, L.M. and Dawson, J.L., "Corrosion Rates from Impedance Measurements: An Introduction," *Brit. Corros. J.*, 15, 20 (1980).